

ME 502 PROJECT 2

CONDENSER

February 15, 2023

Net ID: jiongc2

Name: Jiong Chen

University of Illinois at Urbana-Champaign

Department of Mechanical Engineering

Contents

Abstract	2
Introduction	2
Methods	2
Results and Discussion	10
Conclusions	11
References	21

ABSTRACT

Condenser is a critical part in air conditioner or heat pump system. In this project, a condenser with horizontal flat tubes and louver fins is simulated. The simulation evaluates the thermal performance and the hydraulic performance of the radiator with the finite volume concept. The simulation is accomplished by Python and package CoolProp is used for retrieving the thermal properties. For thermal performance, $\epsilon - NTU$ method is used for calculation of heat transfer rate; empirical correlations are adopted for heat transfer coefficient, and hydraulic pressure drop. Different heat transfer correlations and pressure drop correlations for two-phase refrigerant are discussed. The simulation evaluated the impact of element numbers through the tube to the performance evaluation. Larger mesh size can lead to more accurate result; however, it can also increase computation load. Keep increasing mesh size will result in small improvement of accuracy but more computation work. The best mesh size is determined.

INTRODUCTION

A traditional AC system consists of a condenser, evaporator, compressor and expansion valve. The superheated refrigerant leaves evaporator and enters the compressor. After the compressor, the refrigerant is compressed to a more superheated level. And it enters condenser. In the condenser, refrigerant condenses from superheated level to subcooled level. Usually a system should have around 5°C level of subcooling and superheating.

The refrigerant for the studied condenser is R1234yf. The geometry for the condenser is included in Table 1 and Table 2. Notice that this condenser has two passes. The reason why condenser has two-passes design is that: after the first pass, the vapor quality of the refrigerant flow decreases and will lead to a lower heat transfer coefficient; the second pass has smaller number of tubes than the first pass; so when the flow enters the second pass, the mass velocity increases which leads to higher heat transfer coefficient compensating with higher pressure drop. The simulation condition is included in Table 3.

METHODS

For Methods, it consists of two parts: thermal and hydraulic.

For thermal calculation, air is assumed to be ideal gas, no condensation included. The tube wall thermal resistance is neglected. And the thermal conductivity of metal is assumed

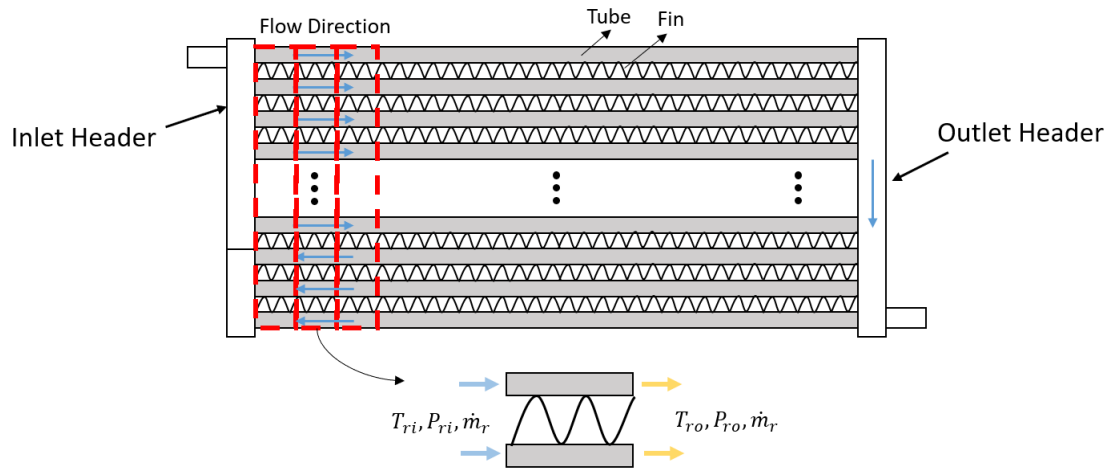


Figure 1: Condenser Schematic

Tube Geometry	Size
N_{slab} : number of slabs (rows), [-]	1
N_{pass} : number of passes in one slab, [-]	2
$L_{tube,pass}$: tube length in one pass, [mm]	650
$N_{tube,pass}$: number of tubes in one pass, [-]	35
t_{wall*} : wall thickness, [mm]	0.35
t_{tube} : tube thickness, [mm]	1.7
D_{tube} : tube depth, [mm]	20
N_{port} : number of ports in one tube, [-]	13
Ra_{tube} : roughness of tube inner surface, [m]	10^{-6}

* t_{wall} : assume all the outer walls and inner walls have the same thickness

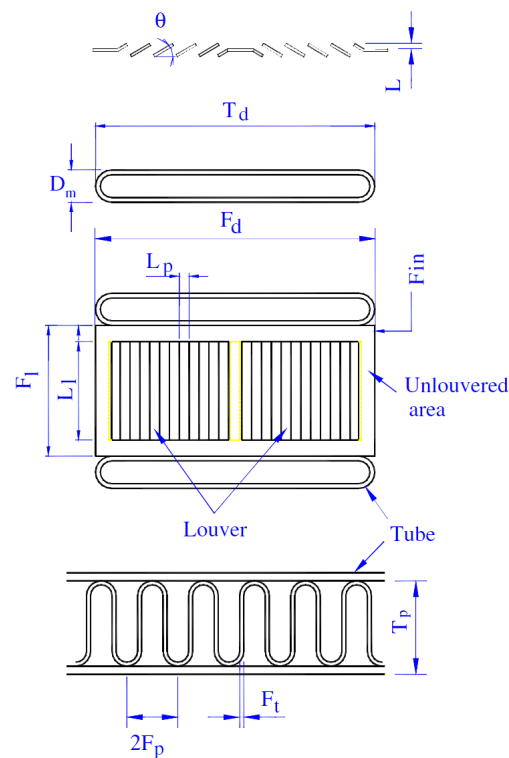
Table 1: Dimensions of the tubes of the radiator

Fin Geometry	Size
θ_{louver} : louver angle, [deg]	20
P_{louver} : louver pitch, [mm]	1.3
L_{louver} : louver length, [mm]	7.2
$N_{louverbank}$: number of louvers sets per fin, [-]	2
h_{fin} : fin height, [mm]	8
t_{fin} : fin thickness, [mm]	0.1
P_{fin} : fin pitch, [mm]	1.4 (18 FPI*)
D_{fin} : Depth of fin, [mm]	20

*FPI: fin per inch

Table 2: Dimensions of the fins of the radiator

Parameter	Value
T_{ri} : refrigerant inlet temperature, [C]	75
$T_{sat,ri}$: refrigerant inlet saturation temperature, [C]	48
\dot{m}_{ref} : refrigerant volumetric flow rate, [g/s]	35
T_{ai} : air inlet temperature, [C]	35
P_{ai} : air inlet pressure, [kPa]	99.5
V_a : air volumetric flow rate, [CFM]	1500

Table 3: Simulation Condition**Figure 2:** Definition of various geometric parameters for corrugated louver fin [1]

to be constant. heat transfer coefficient (htc) for air side and coolant side is calculated according to Chang and Wang's correlation [2], and Nusselt number for laminar flow and Gnielinski correlation for turbulent flow. Since the air inlet flow temperature and pressure are the same for each element, the air side htc only needs to be calculate once with following step:

$$htc_{air} = \rho_{air} \times Vel_{air} \times Cp_{air} \times St \quad (1)$$

$$St = j \times Pr_{air}^{-2/3} \quad (2)$$

$$Vel_{air} = \frac{\dot{m}_a}{\rho_{air} A_{air,free}} \quad (3)$$

$$A_{air,free} = A_{front} - A_{ft,cross} \quad (4)$$

$$A_{ft,cross} = (N_{tube,pass} N_{pass} t_{tube} L_{tube,pass}) - (N_{tube,pass} N_{pass} - 1) L_{tube,pass} P_{fin} h_{fin} t_{fin} \quad (5)$$

The j , j -Colburn factor in equation (2) can be calculated with Chang and Wang's correlation[?], which depends on the geometry of the fin and tube:

$$j = Re_{Lp}^{-0.49} \left(\frac{\theta_{louver}}{90} \right)^{0.27} \left(\frac{P_{fin}}{P_{louver}} \right)^{-0.14} \left(\frac{h_{fin}}{P_{louver}} \right)^{-0.29} \left(\frac{D_{tube}}{P_{louver}} \right)^{-0.23} \left(\frac{L_{louver}}{P_{louver}} \right)^{0.68} \left(\frac{P_{tube}}{P_{louver}} \right)^{-0.28} \left(\frac{t_{fin}}{P_{louver}} \right)^{-0.05} \quad (6)$$

$$Re_{Lp} = \frac{\rho_{air} Vel_{air} P_{louver}}{\mu_{air}} \quad (7)$$

For refrigerant side htc, single-phase condition and two-phase condition are discussed separately.

For single phase: for the fully developed internal laminar flow, Nu is calculated according to Table 4 from Heat Transfer Textbook. Due to complex wall condition, Nu is taken as the average number of uniform heat flux case and uniform wall temperature case. Data interpolation is used to calculate the condition that $\frac{b}{a}$ is not the case in the table. The interpolation method used in the simulation is Python package interpolate with method UnivariateSpline. For the flow $Re_D > 2300$, which is turbulent, Nu can be calculated with Gnielinski correlation [3]:

$$f = (0.79 \ln Re_D - 1.64)^{-2} \quad (8)$$

$$Nu_D = \frac{\frac{f}{8} (Re_D - 1000) Pr}{1 + 12.7 \left(\frac{f}{8} \right)^{1/2} (Pr^{(2/3)} - 1)} \quad (9)$$


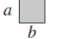
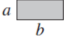
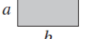
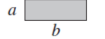
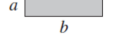
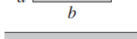
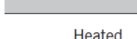
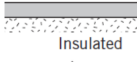

Cross Section	$\frac{b}{a}$	$Nu_D = \frac{HTC \cdot D_h}{k}$	
		(Uniform q_s'')	(Uniform T_s)
	—	4.36	3.66
	1.0	3.61	2.98
	1.43	3.73	3.08
	2.0	4.12	3.39
	3.0	4.79	3.96
	4.0	5.33	4.44
	8.0	6.49	5.60
	∞	8.23	7.54
	∞	5.39	4.86
	—	3.11	2.49

Table 4: Nusselt number for laminar internal flow

$$htc_{ref} = \frac{Nu_D k_{ref}}{D_{h,port}} \quad (10)$$

$$D_{h,port} = \frac{4A_{port}}{P_{port}} \quad (11)$$

$$A_{port} = (N_{port} - 2)(H_{port}W_{port}) + 2((W_{port} - \frac{H_{port}}{2})H_{port} + \pi \frac{H_{port}^2}{4}) \quad (12)$$

$$P_{port} = 2(H_{port} + W_{port})(N_{port} - 2) + 2(H_{port} + 2(W_{port} - \frac{H_{port}}{2})) \quad (13)$$

$$H_{port} = t_{tube} - 2t_{wall} \quad (14)$$

$$W_{port} = (D_{tube} - (N_{port} + 1)t_{wall}) / N_{port} \quad (15)$$

For two-phase refrigerant side heat transfer coefficient, Kim's [9] and Shah's [10] correlations are adopted and inspected in the simulation. For Kim's correlation, the main equation is:

$$h_{tp} = \left(\frac{Nu_3}{Nu_4} \right) h_{tp,cir} \quad (16)$$

For $h_{tp,cir}$, it can be calculated based on the flow regime. Detailed calculation can be found in [9] Table 3. For Shah's correlation, the main equation is:

$$h_l = h_{LT} \left[1 + 1.128x^{0.817} \left(\frac{\rho_L}{\rho_G} \right)^{0.3685} \left(\frac{\mu_L}{\mu_G} \right)^{0.2363} \left(1 - \frac{\mu_G}{\mu_L} \right)^{2.144} Pr_L^{-0.1} \right] \quad (17)$$

The detailed calculation of h_{LT} can be found in [10]. With htc_{air} and htc_{ref} , using $\epsilon - NTU$ method:

$$Q = \sigma C_{min}(T_{ri} - T_{ai}) \quad (18)$$

$$\sigma = 1 - \exp\left(\frac{1}{C_{ratio}} NTU^{0.22} (\exp(-C_{ratio} NTU^{0.78}) - 1)\right) \quad (19)$$

$$NTU = \frac{UA}{C_{min}} \quad (20)$$

$$UA = \frac{1}{R_{air} + \frac{1}{htc_{ref} A_{ref,elem}}} \quad (21)$$

$$R_{air} = \frac{1}{htc_{air} A_{air,elem} \eta} \quad (22)$$

$$T_{ro} = T_{ri} - Q/C_{ref} \quad (23)$$

$$T_{ao} = T_{ai} + Q/C_{air} \quad (24)$$

in equation (20), η is the overall fin efficiency. $A_{air,elem}$ and $A_{ref,elem}$ are air side heat transfer area and refrigerant side heat transfer area for each element respectively. Thus, the heat transfer rate of each element is calculated, and the outlet air temperature, outlet water-EG temperature can be obtained by equation (21) and (22).

For hydraulic performance, Churchill's [4] correlation is adopted for single phase R1234yf and Chang and Wang's [5] Correlation is adopted for air side. The pressure drop of R1234yf consists of static pressure, hydrostatic pressure and dynamic pressure. Consider that all the tubes are horizontal, the hydrostatic pressure can be neglected; for one segment, the velocity of coolant change is negligible under single phase condition so that dynamic pressure can be neglected. The main contribution to pressure drop is static pressure which caused by friction. Pressure drop in tube can be calculated as following:

$$DP_{ref} = DP_{ref,static} = \frac{\partial p}{\partial z_f} \frac{L_{elem}}{D_{h,port}} \frac{G_{ref}^2}{2\rho_{ref}} \quad (25)$$

$$\frac{\partial p}{\partial z_f} = 8 \left(\left(\frac{8}{Re_D} \right)^{12} + \left(\frac{1}{A+B} \right)^{1.5} \right)^{\frac{1}{12}} \quad (26)$$

$$A = (-2.456 \ln^{0.9} \left(\frac{7}{Re_D} \right) + 0.27 \frac{Ra_{tube}}{D_{h,port}})^{16} \quad (27)$$

$$B = \left(\frac{37530}{Re_D} \right)^{16} \quad (28)$$

in equation (23), L_{elem} is the tube length of each element, and G_{ref} is the mass flux of refrigerant in each tube.

For two-phase hydraulic performance of R1234yf, Del Col's [7] correlation and Lopez-Belchi's [8] correlation are inspected in the simulation for calculating the static pressure drop. The main equation for Del Col's correlation is:

$$f_{LO} = 0.046(Re_{LO})^{-0.2} + 0.7RR \times X \quad (29)$$

in which Re_{LO} is the liquid-only Reynolds number, RR is relative roughness of the channel (Ra_{tube}), and the calculation of X can be obtained from the original paper. The static pressure drop can be calculated by:

$$DP_{static} = f_{LO} L_{segment} \quad (30)$$

in which $L_{segment}$ is the tube length for each segment.

The main equation for Lopez-Belchi's correlation is:

$$\left(\frac{dp}{dz} \right)_{tp} = \phi_{liq}^2 \left(\frac{dp}{dz} \right)_{liq} \quad (31)$$

$$\phi_{tp}^2 = 1 + \frac{C}{X} + \frac{1}{X^2} \quad (32)$$

$$\left(\frac{dp}{dz} \right)_{liq} = \frac{G^2(1-x)^2}{2D\rho_{liq}} f_{liq} \quad (33)$$

$$\left(\frac{dp}{dz} \right)_{gas} = \frac{G^2 x^2}{2D\rho_{gas}} f_{gas} \quad (34)$$

Notice that for X in equation (30), the calculation is different from Del Col's X . And the calculation of f_{liq} and f_{gas} can be obtained from the original literature. The accelerational pressure drop in two-phase becomes important and non-negligible. It can be calculated with:

$$DP_{acc} = G^2(B - A) \quad (35)$$

$$A = \frac{x_i^2}{\rho_v \alpha_i} + \frac{(1-x_i)^2}{\rho_l (1-\alpha_i)} \quad (36)$$

$$B = \frac{x_o^2}{\rho_v \alpha_o} + \frac{(1 - x_o)^2}{\rho_l (1 - \alpha_o)} \quad (37)$$

in which α is void fraction.

Air side pressure drop is calculated by a equation set provided by Chang and Wang [?]:

$$f = f_1 f_2 f_3 \quad (38)$$

When $Re_{Lp} < 150$:

$$f_1 = 14.39 Re_{Lp}^{-0.805 \frac{P_{fin}}{D_{fin}}} \ln^{3.04} \left(1 + \frac{P_{fin}}{P_{louver}} \right) \quad (39)$$

$$f_2 = \ln^{-1.435} \left(\left(\frac{t_{fin}}{P_{fin}} \right)^{0.48} + 0.9 \right) \left(\frac{D_{h,port}}{P_{louver}} \right)^{-3.01} \ln^{-3.01} (0.5 Re_{Lp}) \quad (40)$$

$$f_3 = \left(\frac{P_{fin}}{L_{louver}} \right)^{-0.308} \left(\frac{D_{fin}}{L_{louver}} \right)^{-0.308} \exp \left(-0.1167 \frac{P_{tube}}{h_{fin}} \right) \theta_{louver}^{0.35} \quad (41)$$

When $150 < Re_{Lp} < 5000$:

$$f_1 = 4.97 Re_{Lp}^{0.6049 - 1.064/\theta^{0.2}} (\ln((t_{fin}/P_{fin})^{0.5} + 0.9))^{-0.527} \quad (42)$$

$$f_2 = ((D_{h,port}/P_{louver}) \ln(0.3 Re_{Lp}))^{-2.966} (P_{fin}/L_{louver})^{-0.7931 (P_{tube}/h_{fin})} \quad (43)$$

$$f_3 = (P_{tube}/t_{tube})^{-0.0446} (\ln(1.2 + (P_{louver}/P_{fin})^{1.4}))^{-3.553} \theta_{louver}^{-0.477} \quad (44)$$

The frictional factor f can also be expressed as:

$$f = \frac{A_c \rho_m}{A \rho_1} \left[\frac{2 \rho_1 D P_{air}}{G_c^2} - (K_c + 1 - \sigma^2) - 2 \left(\frac{\rho_1}{\rho_2} - 1 \right) + (1 - \sigma^2 - K_e) \frac{\rho_1}{\rho_2} \right] \quad (45)$$

where G_c is the air mass flux after contraction; A_c is the free flow area, A is total surface area; ρ_1 and ρ_2 represents inlet and outlet air density respectively and ρ_m is the average density of inlet and outlet air; K_c and K_e are entrance and exit loss coefficients (the abrupt contraction and expansion coefficients) which are evaluated from Kays and London [6] at $Re_{Dh} = \infty$. With equation (33) and (34), we can calculate air side pressure drop. In this part, since the outlet density cannot be determined with only tempearture, iteration is required.

In each tube segment, the simulation algorithm is: firstly, determine whether or not refrigerant is under two-phase condition; secondly, calculate heat transfer using $\epsilon - NTU$ method; thirdly, find pressure drop for both air-side and refrigerant-side; finally, generate output which will be the input of next segment. By calculating one tube's thermal and hydraulic

performance, the total energy transfer rate of the radiator is:

$$Q_{tot} = \text{sum}(Q_{elem}) \quad (46)$$

the outlet air temperature and pressure are approximated as the average of all the air outlet:

$$T_{ao} = \text{ave}(T_{ao,elem}) \quad (47)$$

$$P_{ao} = \text{ave}(P_{ao,elem}) \quad (48)$$

the water-EG outlet temperature and pressure are taken as the calculated tube outlet temperature and pressure.

RESULTS AND DISCUSSION

The simulation is conducted with the number of segments ranging from 1 to 80. Lopez's correlation and Shah's correlation is used in the simulation. Detailed thermal and hydraulic performance of the condenser are shown in figure 3 to figure 9. Table 5 includes the outlet condition of refrigerant and air. In the figures, the black dashed line at segment equals 60 represents the refrigerant enters the second pass. Figure 3 shows that after around 13 or 14 segments, the refrigerant enters two-phase condition and after around 80 segments, the refrigerant is subcooled. In Figure 4, for two-phase region, refrigerant has higher pressure drop in second pass, which meets our expectation and is the compensation of increasing heat transfer coefficient as shown in Figure 8. Figure 6 and Figure 7 shows the air side performance. In Figure 8, heat transfer coefficient in two-phase region is larger than single-phase region. From Figure 10 to Figure 12, they are comparison between two different HTC correlations for two-phase R1234yf. And Figure 13 to Figure 15 are comparison between different static pressure drop correlations for two-phase R1234yf. Notice that different correlations have similar trend, which makes simulation reasonable. However, there are difference between the calculated value from different correlations. Thus, simulation is not always reliable. And choosing correlation correctly before simulation is very important.

Figure 16 to Figure 21 are the impact of segment number on the simulation results. The simulation results converges after the segment number is larger than 40 even 50. The summarized performance of condenser is calculated under segment number equals 60 so that the condenser is converged. Notice that when segment number equals to one, which is the lumped parameter analysis, simulation result has significant error. For two-phase simulation,

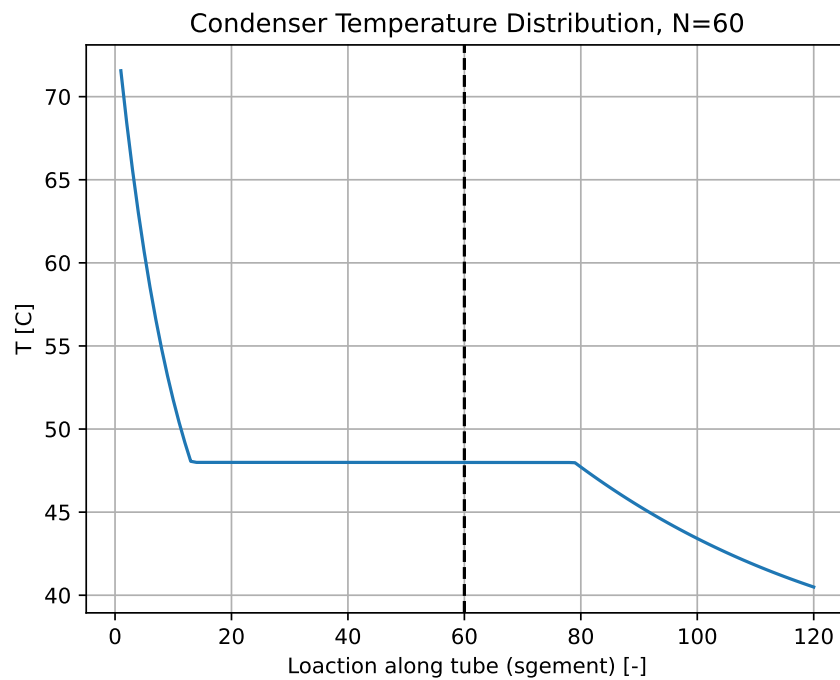


Figure 3: Temperature distribution along tube, $N_{segment} = 60$

Parameter	Value
T_{ro} : refrigerant outlet temperature, [C]	40.49
P_{ro} : refrigerant outlet pressure, [kPa]	1240.69
T_{ao} : air outlet temperature, [C]	41.22
P_{ao} : air outlet pressure, [kPa]	99.48
Q_{tot} : total heat transfer rate, [kW]	5.86

Table 5: Overall performance of radiator, $N_{segment} = 40$

lumped parameter analysis is not applicable.

CONCLUSIONS

This project studied about simulation for condenser thermal and hydraulic performance. The impact of mesh size is discussed. There should be a optimized mesh size for each simulation with consideration of accuracy and computation time. In addition, choosing appropriate correlations are crucial. Different correlations can lead to different simulation result. The simulation with different correlations may have similar trend, but the results can be different. Simulation is not always reliable and experiment validation is necessary.

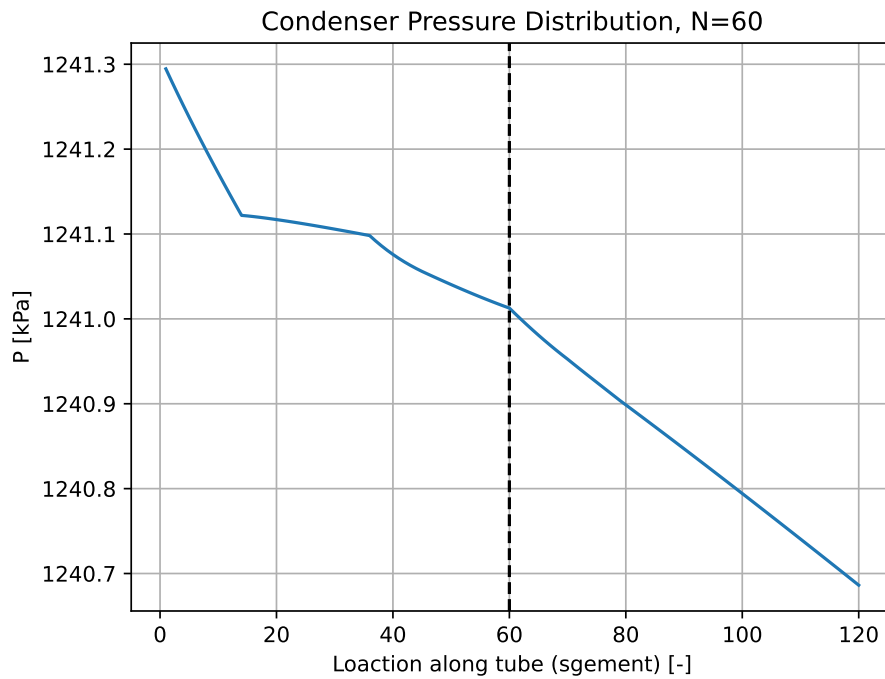


Figure 4: Pressure distribution along tube, $N_{segment} = 60$

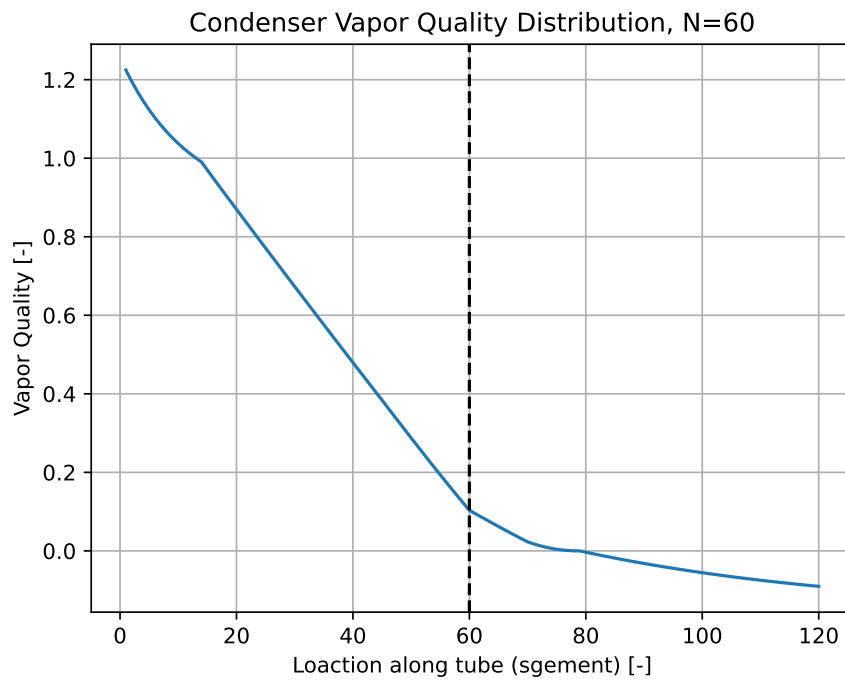


Figure 5: Vapor Quality distribution along tube, $N_{segment} = 60$

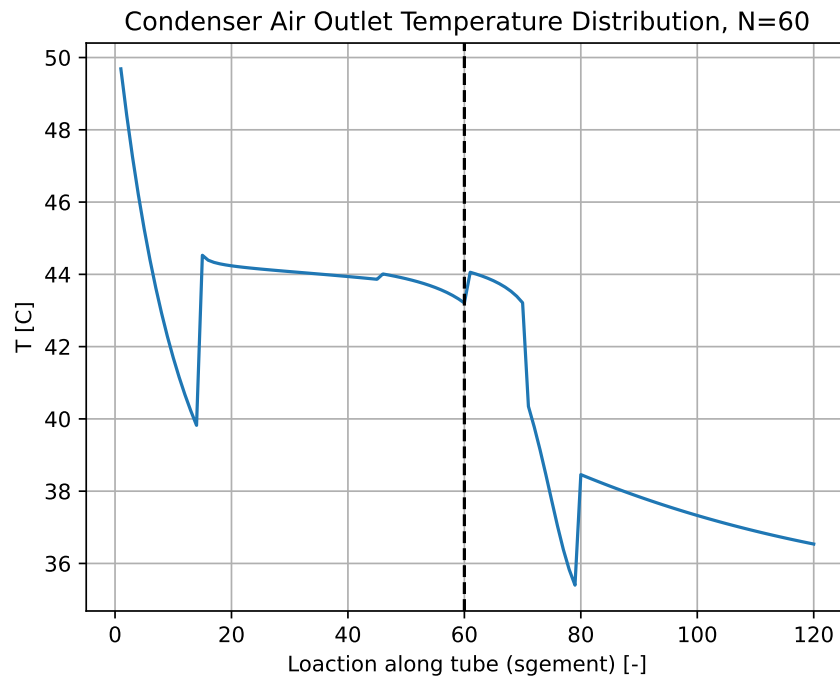


Figure 6: Air outlet temperature distribution along tube, $N_{segment} = 60$

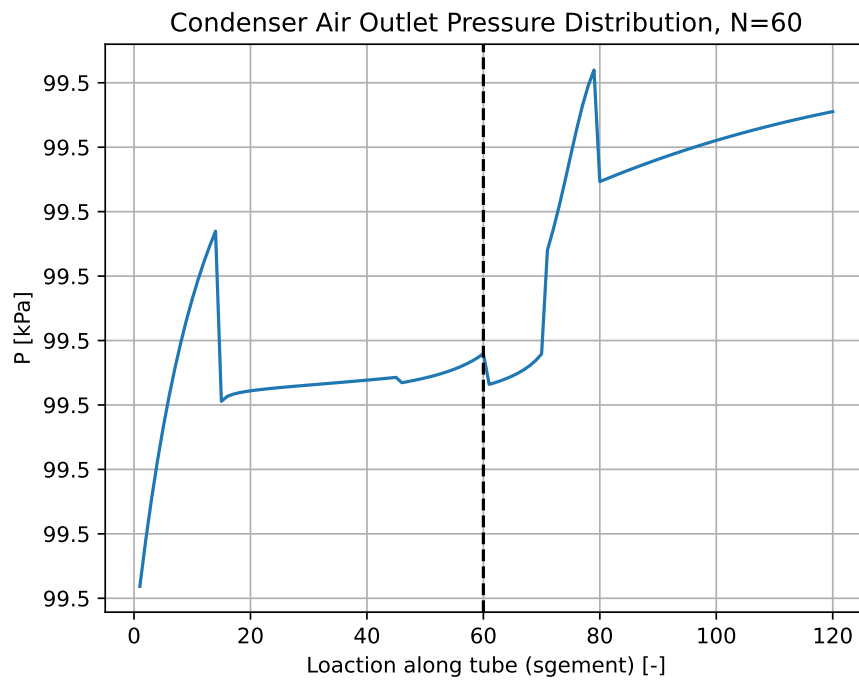


Figure 7: Air outlet pressure distribution along tube, $N_{segment} = 60$

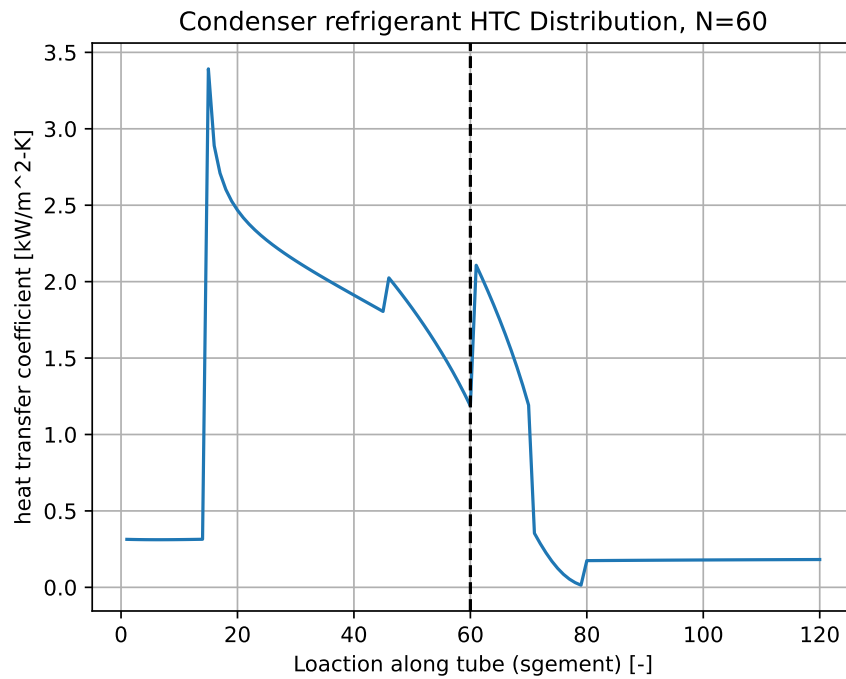


Figure 8: Heat transfer coefficient distribution along tube, $N_{segment} = 60$

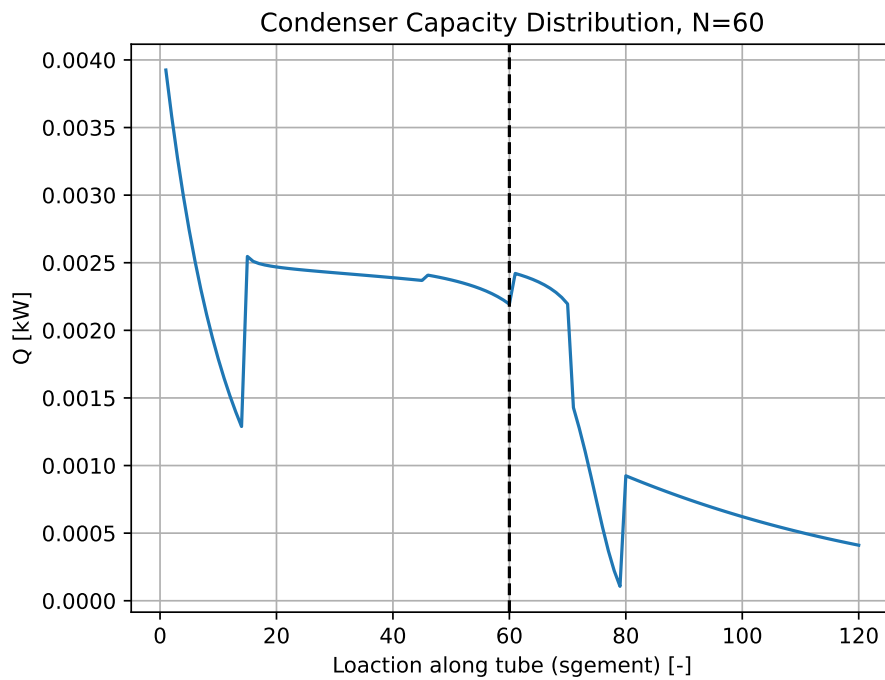


Figure 9: Heat transfer rate distribution along tube, $N_{segment} = 60$

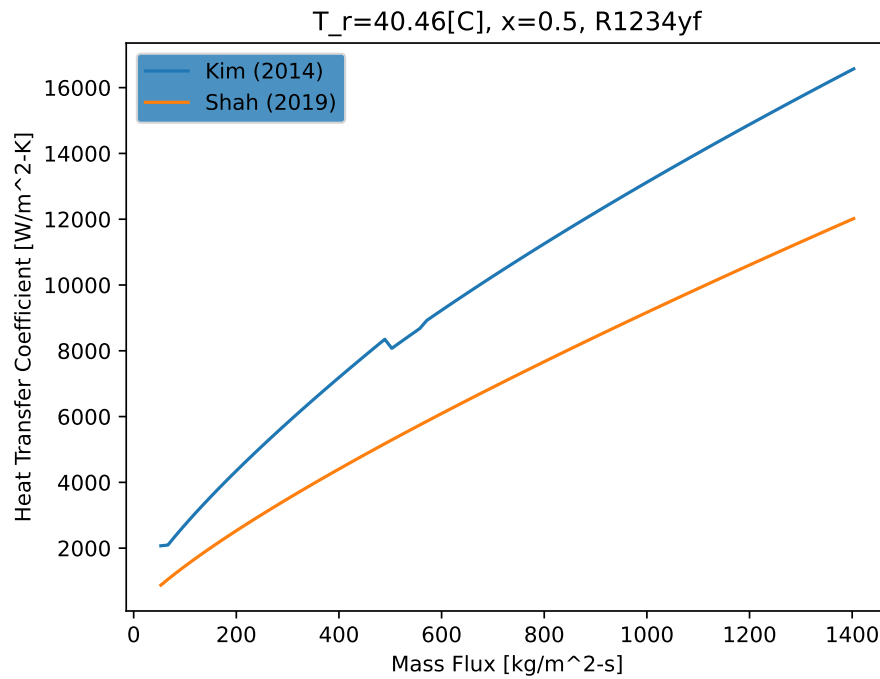


Figure 10: two-phase, HTC correlation comparison with different mass velocity

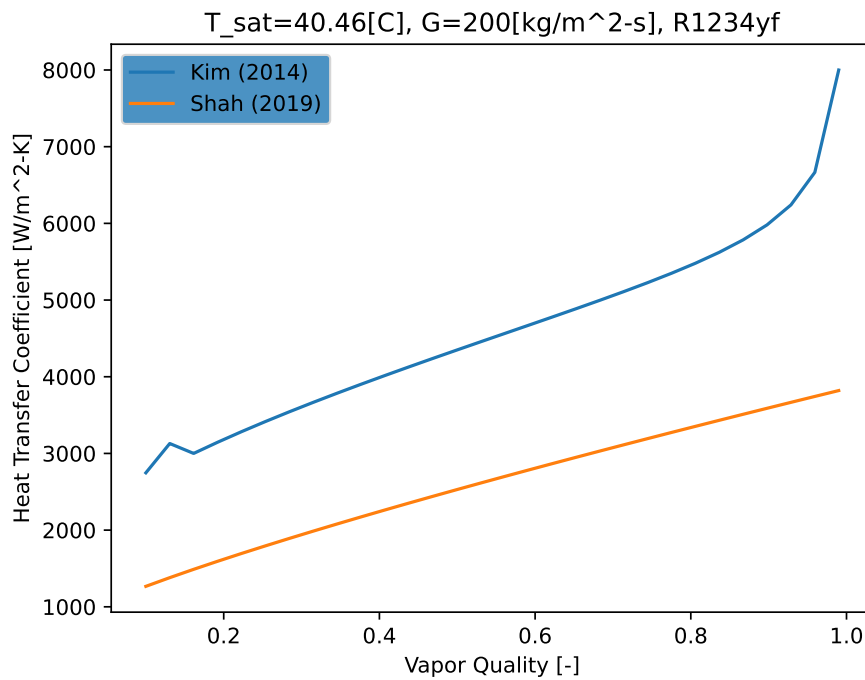


Figure 11: two-phase, HTC correlation comparison with different vapor quality

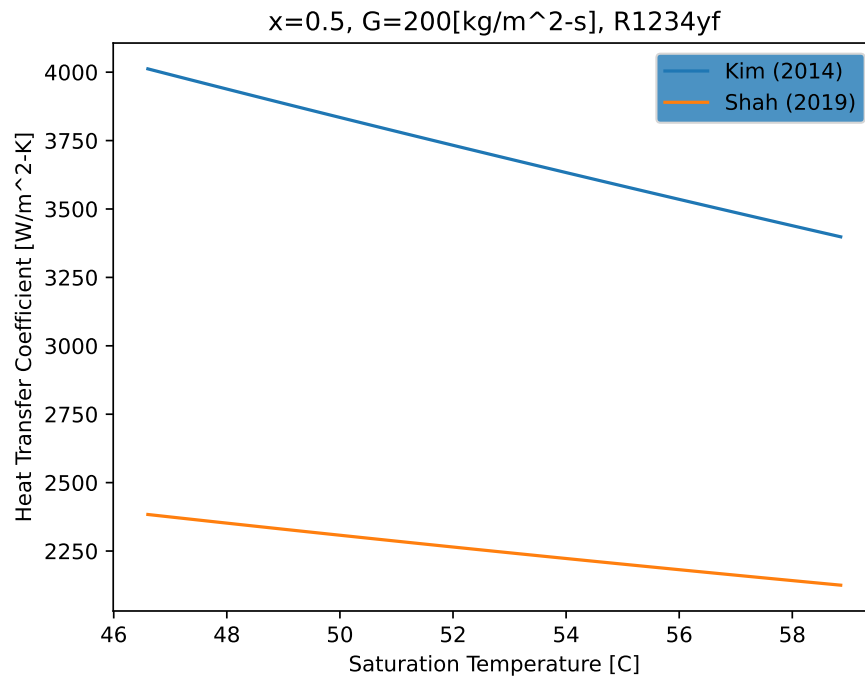


Figure 12: two-phase, HTC correlation comparison with different saturation temperature

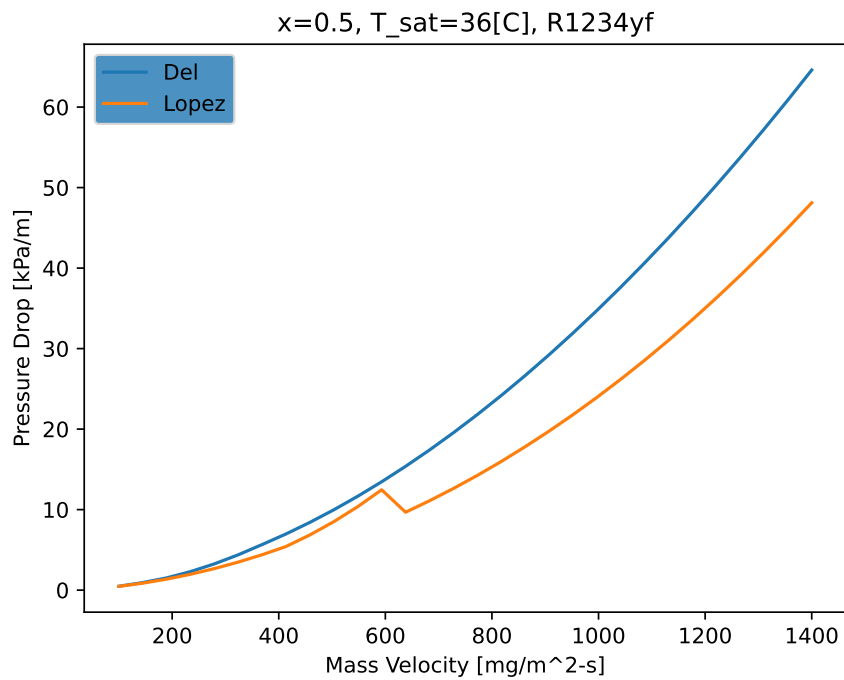


Figure 13: two-phase, pressure drop correlation comparison with different mass velocity

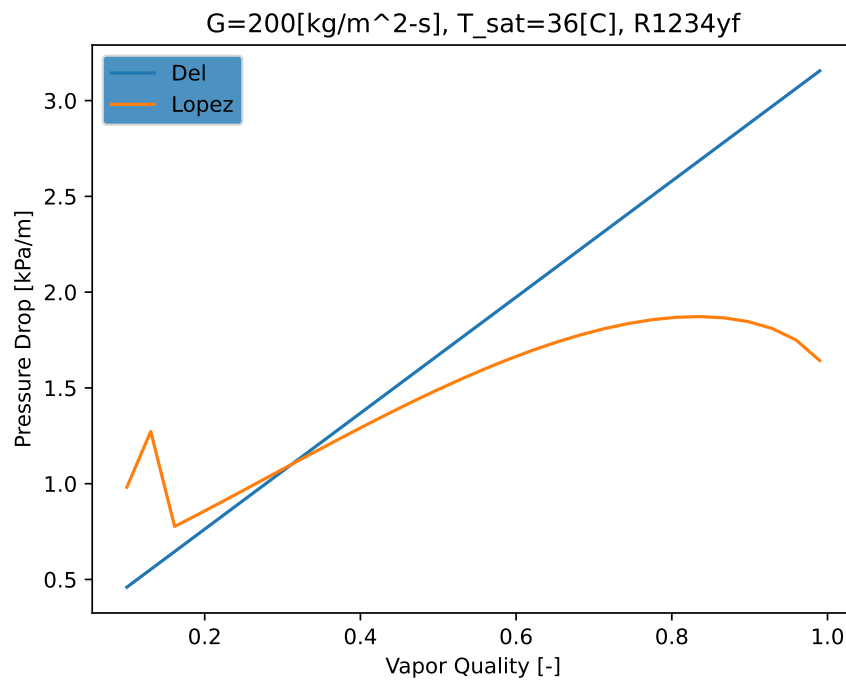


Figure 14: two-phase, pressure drop correlation comparison with different vapor quality

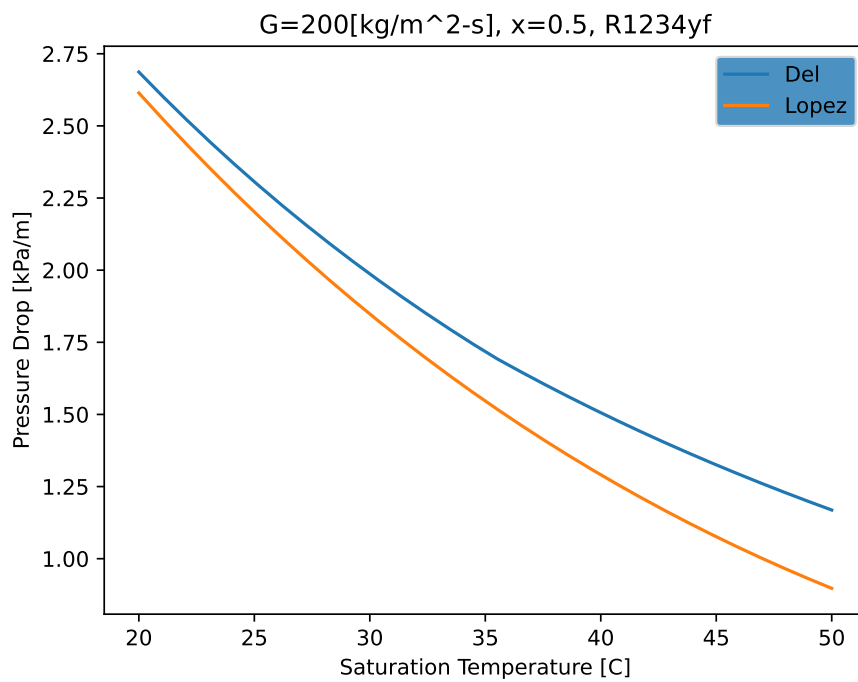


Figure 15: two-phase, pressure drop correlation comparison with different saturation temperature

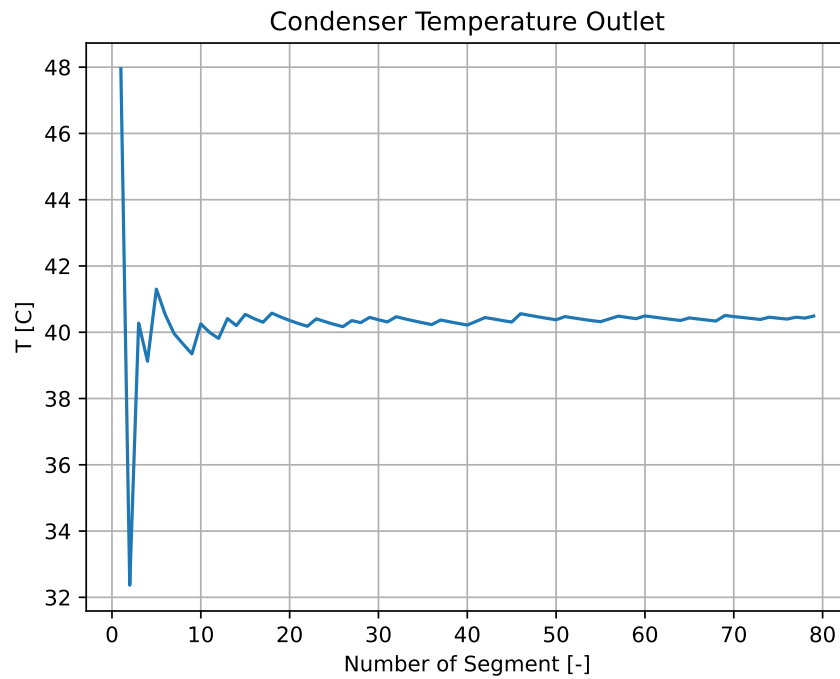


Figure 16: Segment number impact, refrigerant outlet temperature

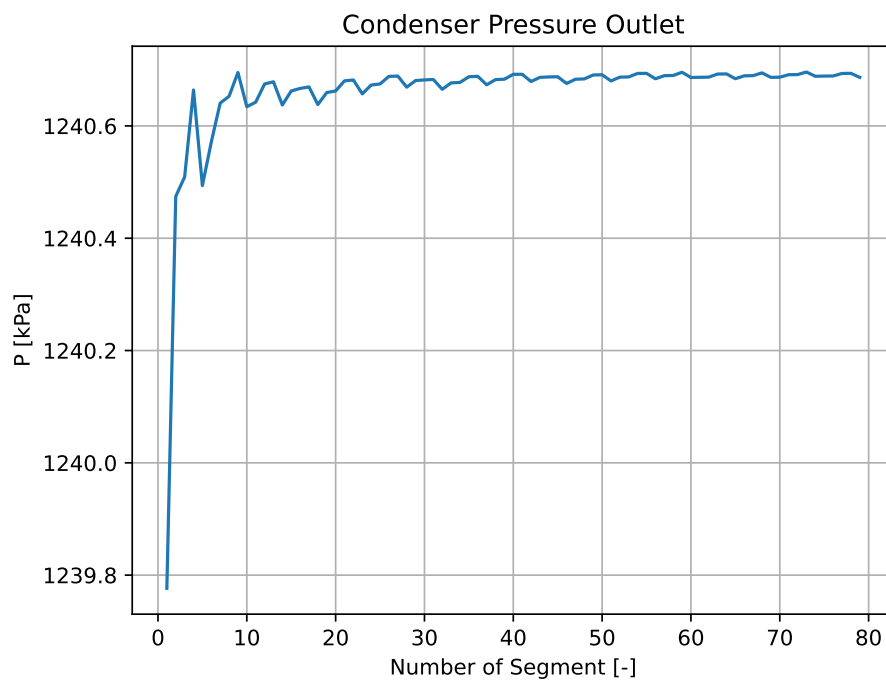


Figure 17: Segment number impact, refrigerant outlet pressure

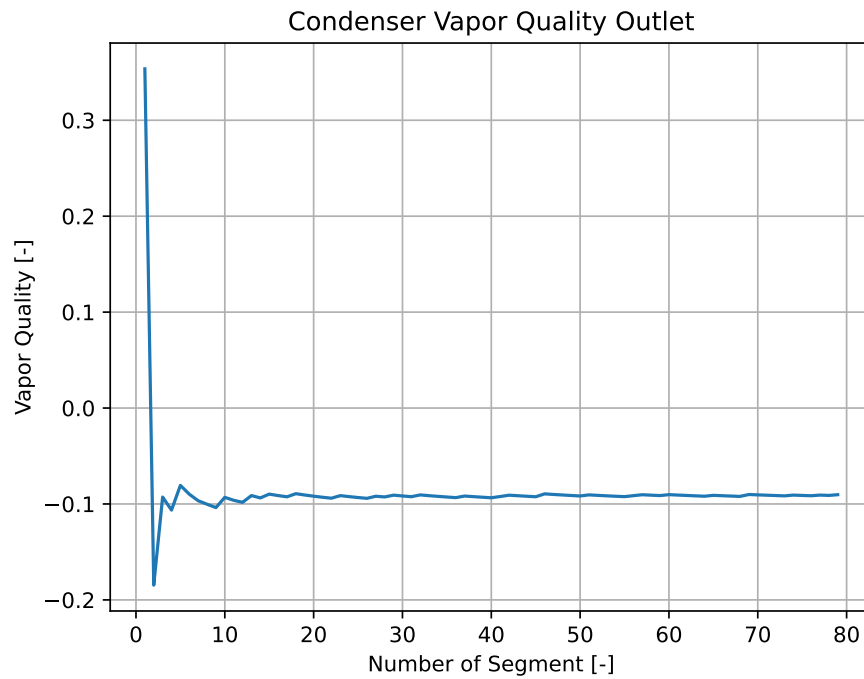


Figure 18: Segment number impact, refrigerant outlet vapor quality

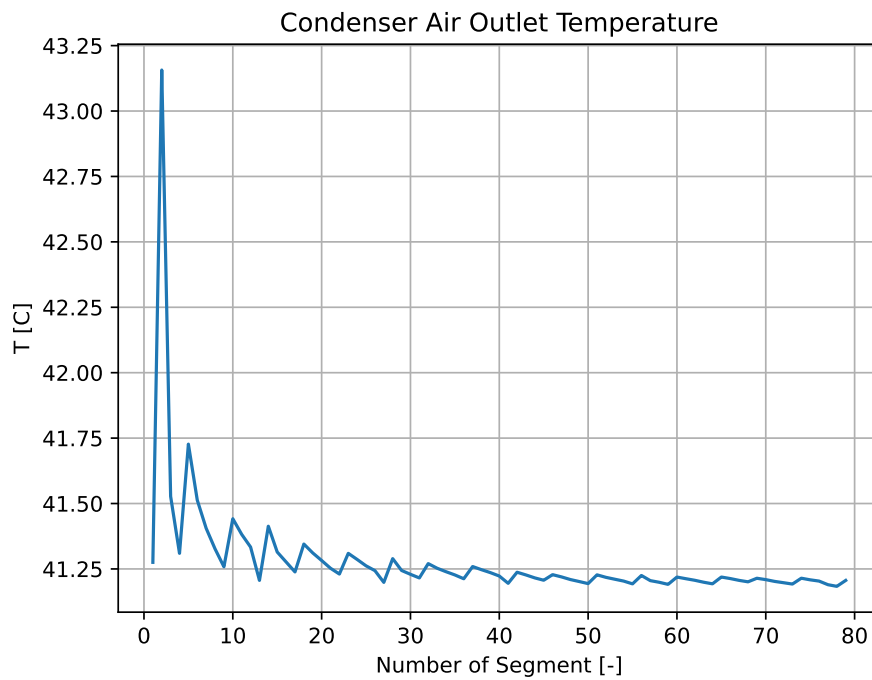


Figure 19: Segment number impact, air outlet temperature

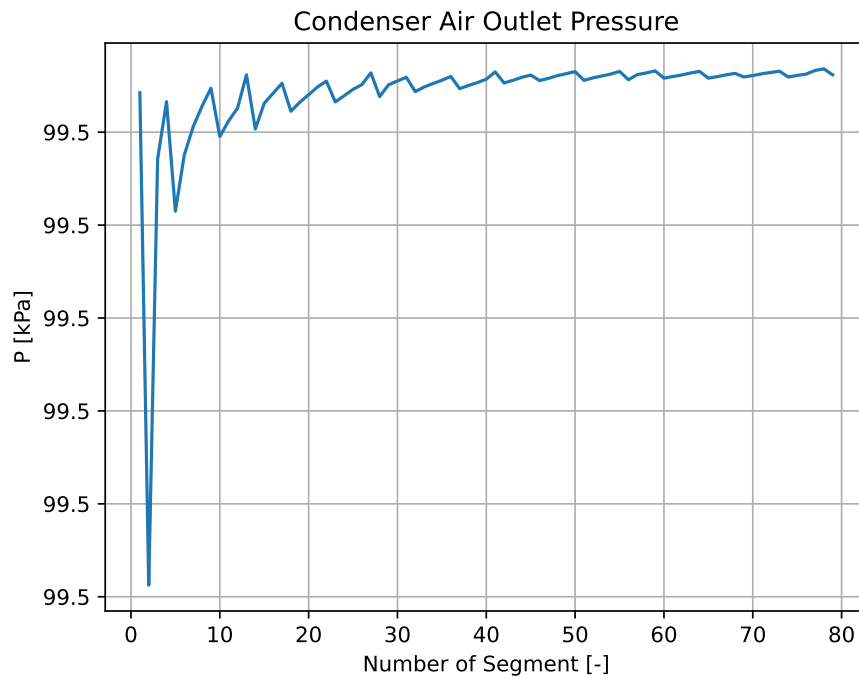


Figure 20: Segment number impact, air outlet pressure

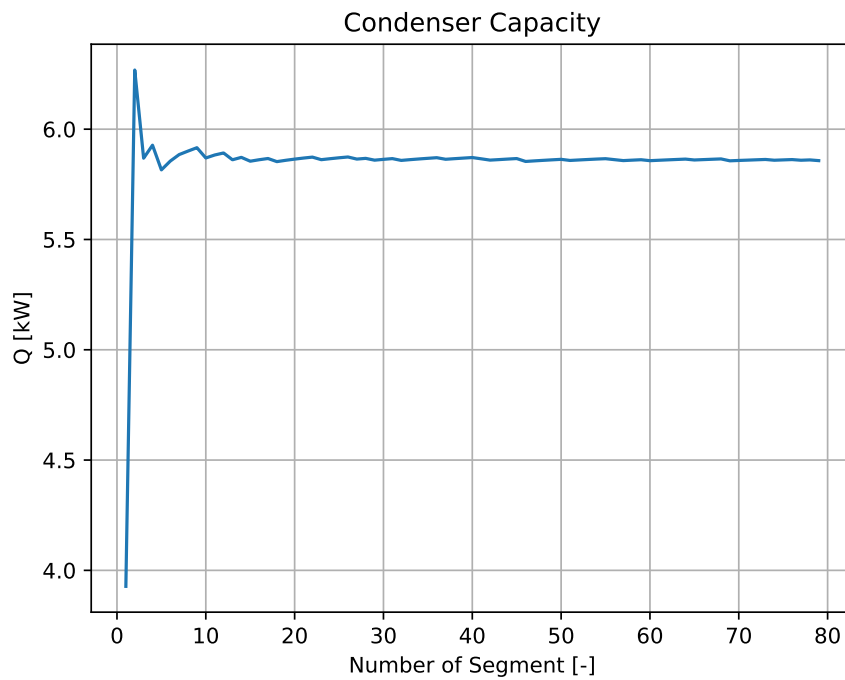


Figure 21: Segment number impact, condenser capacity

REFERENCES

- [1] Chang, Y-JY-J., et al. "A generalized friction correlation for louver fin geometry." *International journal of heat and mass transfer* 43.12 (2000): 2237-2243.
- [2] Chang, Yu-Juei, and Chi-Chuan Wang. "Air side performance of brazed aluminum heat exchangers." *Journal of Enhanced Heat Transfer* 3.1 (1996).
- [3] Gnielinski, Volker. "New equations for heat and mass transfer in the turbulent flow in pipes and channels." *NASA STI/recon technical report A 41.1* (1975): 8-16.
- [4] Churchill, Stuart W. "Friction-factor equation spans all fluid-flow regimes." (1977).
- [5] Chang, Y-JY-J., et al. "A generalized friction correlation for louver fin geometry." *International journal of heat and mass transfer* 43.12 (2000): 2237-2243.
- [6] Kays, William Morrow, and Alexander Louis London. "Compact heat exchangers." (1984).
- [7] Del Col, Davide, et al. "Experiments and updated model for two phase frictional pressure drop inside minichannels." *International journal of heat and mass transfer* 67 (2013): 326-337.
- [8] Lopez-Belchi, Alejandro, et al. "Experimental condensing two-phase frictional pressure drop inside mini-channels. Comparisons and new model development." *International Journal of Heat and Mass Transfer* 75 (2014): 581-591.
- [9] Kim, Sung-Min, and Issam Mudawar. "Review of databases and predictive methods for heat transfer in condensing and boiling mini/micro-channel flows." *International Journal of Heat and Mass Transfer* 77 (2014): 627-652.
- [10] Shah, Mirza M. "Improved correlation for heat transfer during condensation in conventional and mini/micro channels." *International Journal of Refrigeration* 98 (2019): 222-237.